CLEO TALK 04-42

FIRST RESULTS FROM CLEO-c

John M Yelton
Phys. Dept, U.of Florida, Gainesville, FL 32611-8440
On Behalf of the CLEO Collaboration

Heavy Quarks and Leptons, San Juan, Puerto Rico
June 4th, 2004

Abstract

We present the first results from the CLEO-c experiment. CLEO-c is a new detector configuration running at the charmonium and charm meson threshold energies at the Cornell Electron Storage Ring. Here, we show the first results on data taken at the $\psi(3770)$ resonance. In particular, we present the first significant signal of the decay $D^+ \to \mu\nu$ which leads to a measure of the D meson decay constant f_D.

1 Introduction

The summer of 2004 is an exciting time for the CLEO collaboration. For some years, we have been showing Monte Carlo simulations of the data we will be able to present using the CLEO-c detector. Now, for the first time, we can show results that in many aspects match the simulations. In particular, we see that the background estimates were reasonable, and will not preclude the measurements we hope to make. I stress that all the data and results presented here are preliminary, and are taken using a fraction of the luminosity we intend to accumulate.

2 The CLEO-c Detector and the CESR-c Accelerator

The CLEO collaboration has been taking data at the Cornell Electron Storage Ring since 1980. The latest detector configuration is known as CLEO-c, where the "c" denotes charm, as it incorporates changes to make it more suitable for taking data at around the charm threshold energies. CLEO-c retains the CLEO III main drift chamber and particle ID system (Ring Imaging Cherenkov counters (RICH)[1] and energy loss (dE/dx) measurements), and the CsI crystal calorimeter for photon and electron detection that was built for CLEO II[2]. The main change from CLEO III is the replacement of the silicon vertex detector with a six-layer, all-stereo, inner drift chamber[3]. This is known as the "ZD", as its primary role is the measurement of the tracks in the "Z" (along the beam) direction. The ensemble is centered in the CLEO solenoidal magnet, which is run at 1.0 Tesla, rather than 1.5T which was used for CLEO III. The lower magnetic field reduces the fraction of curling tracks.

The CESR accelerator has been modified to enable the changing physics plans. Superconducting wiggler magnets are being added to the machine lattice to help damp the synchrotron radiation. Six such wigglers were already operational for the data run discussed here; the rest have just been installed and will be operational in Fall 2004.

3 The CLEO-c Data Set

We have collected 3 pb^{-1} of $\psi(2S)$ data in CLEO-c. Together with some earlier exploratory running (before the new inner drift chamber was installed), we have a total of 5.5 pb^{-1} of $\psi(2S)$ data which include about 3 million $\psi(2S)$ decays. We also have 20 pb^{-1} of continuum data taken at $\sqrt{s} \simeq 3.67$ GeV, just below the $\psi(2S)$. Perhaps the most exciting new data sample is ≈ 57 pb^{-1} taken on the $\psi(3770)$ resonance which yields $D\bar{D}$ pairs, and this talk will concentrate on this last sample. The $\psi(2S)$ results are being presented in another talk.

These datasets are only the start of the CLEO-c program. The run-plan presently calls for a massive 3 fb^{-1} of $\psi(3770)$ running, a factor of around 60 greater than presented here. We stress that this goal is contingent on CESR being able to quickly reach its design luminosity of $\approx 3 \times 10^{32} cm^{-2} s^{-1}$, which is a factor of six higher than has been achieved so far. The physics run-plan is deliberately flexible so that it can change in reaction to the results obtained. The planned final dataset would correspond to arround 18,000,000 $D\bar{D}$ decays, and around 3,600,000 *tagged* D decays which is 310 times larger than the MARKIII collaboration and around 170 times larger than that obtained by BES.

After the $\psi(3770)$ data, the plan calls for 3 fb^{-1} running at the $D_s^+ D_s^-$ threshold, giving maybe 300,000 *tagged* D_s decays (130 times the BES sample). Fall 2006 will give the opportunity of running at the J/ψ with maybe a billion events collected! Details of the CLEO-c program may be found elsewhere[4].

4 The Physics at the $\psi(3770$

The main decay of the $\psi(3770)$ is into $D\bar{D}$ mesons. However, the total cross-section also includes a large (and not well understood) continuum component, the radiative tail of the $\psi(2S)$, and maybe some other processes as yet unexplored. Using the data taken at, and below, the $\psi(2S)$ we are studying the first

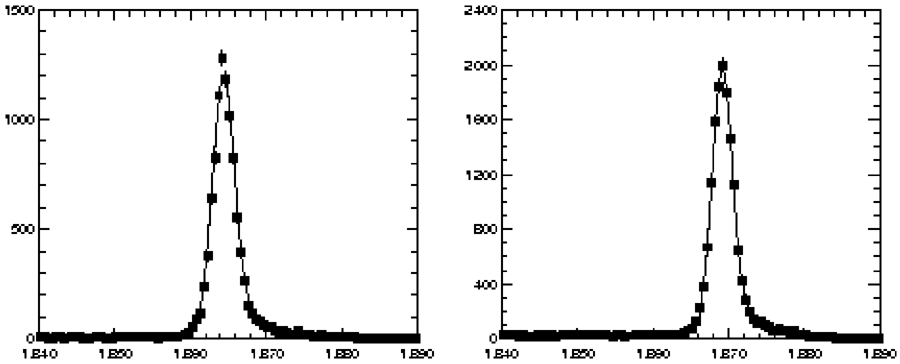

Figure 1: *Beam-constrained mass distributions for a)* $D^0 \rightarrow K^-\pi^+$*, and b)* $D^+ \rightarrow K^-\pi^+\pi^+$

two of these. To know how many D mesons we will eventually be able to reconstruct, we need to know the cross-section into D pairs, that is $(\sigma \rightarrow D\bar{D})$ at E=3.77 GeV. MARKIII[5] measured the observed cross section to be (5.0 ± 0.5) nb. Recently BES II[6], using 17 pb^{-1} measured $(5.78 \pm 0.11 \pm 0.38)$ nb. In the BES method, the cross-section depended upon the value for the branching fraction in the final state under study. Here, we present a double-tag method (along the lines of that used by MARK III) to find a value of $\sigma(e^+e^- \rightarrow D\bar{D})$ independent of any branching fraciton measurement.

4.1 General Analysis Techniques

Good $K - \pi$ separation is obtained by dE/dx up to momenta of around 600 MeV/c. For higher momentum particles we combine RICH information with the dE/dx. In several analyses, we find K_s^0 candidates from their displaced vertices, and reconstruct π^0 mesons from two γ signatures in the CsI calorimeter.

To find D mesons from the $\psi(3770)$, we first calculate the energy of the D and compare with the beam energy. If the two values are consistent, we calculate the beam-constrained mass $M_{BC} = \sqrt{(E_{BEAM}^2 - p(D)^2)}$. The resolution of this quantity is in many cases limited only by the energy spread in the beam. The signal to noise ratio in such a plot is very good, especially in the golden decay modes $D^0 \rightarrow K^-\pi^+$ and $D^+ \rightarrow K^-\pi^+\pi^+$ (Fig. 1) which show spectacularly clean signals.

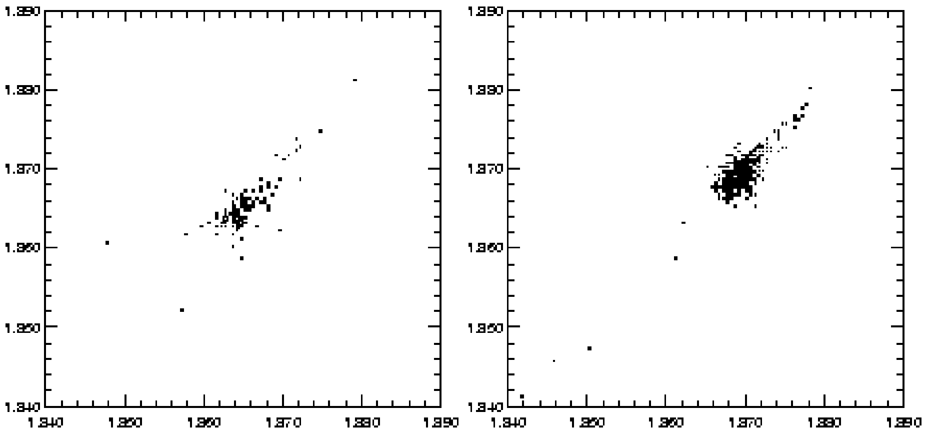

Figure 2: *Beam-constrained mass plots for double tags from* $D^0 \to K^-\pi^+, \bar{D}^0 \to K^+\pi^-$ *(left) and* $D^+ \to K^-\pi^+\pi^+, D^- \to K^+\pi^-\pi^-$ *(right).*

4.2 Double-tag Method to Measure $\sigma(e^+e^- \to D\bar{D}$

Comparing single and double tag yields allows one to easily extract the total $D\bar{D}$ cross-section independently of branching ratios. The number of single D tags, S, in a given mode is $S = 2N_{D\bar{D}}B\epsilon_1$, where the variables denote the number of $D\bar{D}$ pairs produced, the branching fraction of the mode, and the efficiency, respectively. The number of double tags, D, in a given mode is $D = 2N_{D\bar{D}}B^2\epsilon_2$, where $\epsilon_2 \simeq \epsilon_1^2$ is the efficiency for finding both tags. One can then determine the cross section as $\sigma_{D\bar{D}} = S^2/(4DL)$, where L in the integrated luminosity. The branching ratio cancels, as does most of the efficiency (with $\epsilon_2 \neq \epsilon_1^2$ treated as a systematic error).

Table 1 shows the preliminary results from this analysis. We note that our results are consistent with, but a little higher than, previous results on this subject. This is good news for CLEO-c because it implies a larger number of D mesons will be produced. The largest systematic uncertainty is due to the luminosity measurement.

Table 1: *Cross sections of the* $\psi(3770 \to D\bar{D}$.

	$\sigma(D^+D^-)$	$\sigma(D^0\bar{D}^0$	$\sigma(D\bar{D})$
CLEO-c	$2.58 \pm 0.15 \pm 0.16$	$3.93 \pm 0.42 \pm 0.23$	$6.51 \pm 0.44 \pm 0.39$
BES[6]	$2.52 \pm 0.07 \pm 0.23$	$3.26 \pm 0.09 \pm 0.26$	$5.78 \pm 0.11 \pm 0.38$
MARK III[5]	2.1 ± 0.3	2.9 ± 0.4	5.0 ± 0.5

5 Results Using D-Tagging

The remainder of the analyses we will present here, depend on the technique of "D-tagging". That is, by reconstructing one D in the event, we know that another D of a particular charge and flavor, must exist in the remainder of the event. The net-tagging efficiency from a combination of D modes is of the order of 20%, and the expectation is that from the full dataset we will be able to tag several million events in this way.

Tagging can be used to find absolute branching fractions not only of hadronic decays, but semi-leptonic and even purely leptonic decays that cannot be fully reconstructed.

5.1 Determination of f_D from $D^+ \to \mu^+\nu_\mu$ Decay

The leptonic decay width of a pseudoscalar meson, such as the D^+, is proportional constant: $\Gamma_{\ell\nu} \propto f_D^2$. The decay constant f_D is related to the quarks annihilation rate via the short-distance weak interaction. The same parameter enters the box diagram of neutral meson mixing (e.g., f_D for $D^0 \leftrightarrow \bar{D}^0$, or f_B for $B^0 \leftrightarrow \bar{B}^0$). In particular, f_B is needed to extract the CKM matrix element information from the already precise B mixing data; f_{B_s} will be needed once B_s mixing is observed. Lattice guage theories connect the decay constants in the D and B regimes.

We search for $D^+ \to \mu^+\nu_\mu$ decays in events where a D tag is present. For this analysis we augment the $K^-\pi^+\pi^+$ events with four other decay modes, $K_s^0\pi^+, K_s^0\pi^+\pi^0, K_s^0\pi^+\pi^+\pi^0$, and $K^0\pi^+\pi^-\pi^+$. We then require that the rest of the event have exactly one charged track consistent with a muon hypothesis (based on energy deposit in the CsI calorimeter) and relatively little extra energy in unmatched (to tracks) calorimeter showers. We calculate for the candidate muon the *missing mass* squared $MM^2 = (E_{bm} - E_\mu)^2 - (-\vec{P}_{tag} - \vec{p}_\mu)^2$ which will peak at zero for signal.

Backgrounds include $\pi^+\pi^0$ events which peak nearby in MM^2 and sometimes survive the calorimeter activity veto, combinatorics from continuum, $K^0\pi^+$ events, and $D^0\bar{D}^0$ events.

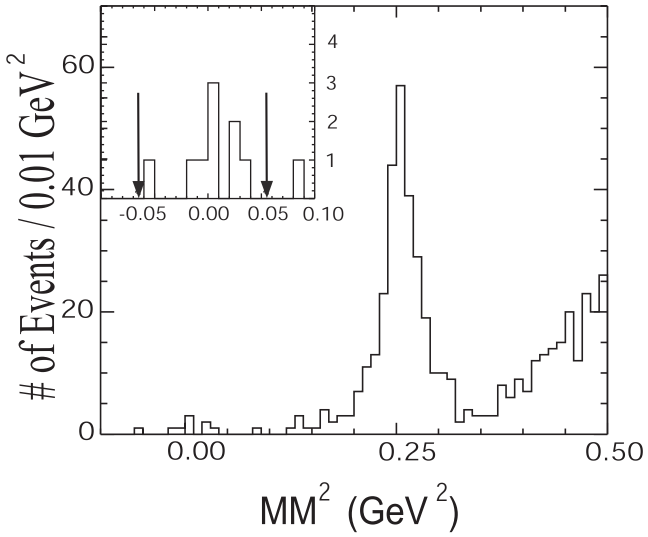

Figure 3: Missing-mass-squared spectra of $D^+ \to \mu^+\nu_\mu$ candidates.

We find 9 events within a 2σ window in MM^2 (see Fig. 3), with a predicted background of 0.67 ± 0.24 events. This has a high significance and gives $\mathcal{B}(D^+ \to \mu^+\nu_\mu) = (4.57 \pm 1.66 \pm 0.41) \times 10^{-4}$, which can be combined with the known D^+ lifetime to extract $f_D = (230 \pm 42 \pm 10)$ MeV. This is consistent with the theoretical expectations, for instance the UKQCD lattice result[7] of $210 \pm 10^{+17}_{-16}$ MeV. The most significant systematics include the muon efficiency (5%) and background level (7.4%). This result is clearly statistics limited; more data will also assist some systematic studies.

6 Inclusive $D \to Xe\nu_e$ Decays

Improved measurements of inclusive lepton spectra from charm mesons are of considerable interest. The integrated spectra providing the inclusive branching fraction, and the shape is also of interest. We concentrate on electrons due to

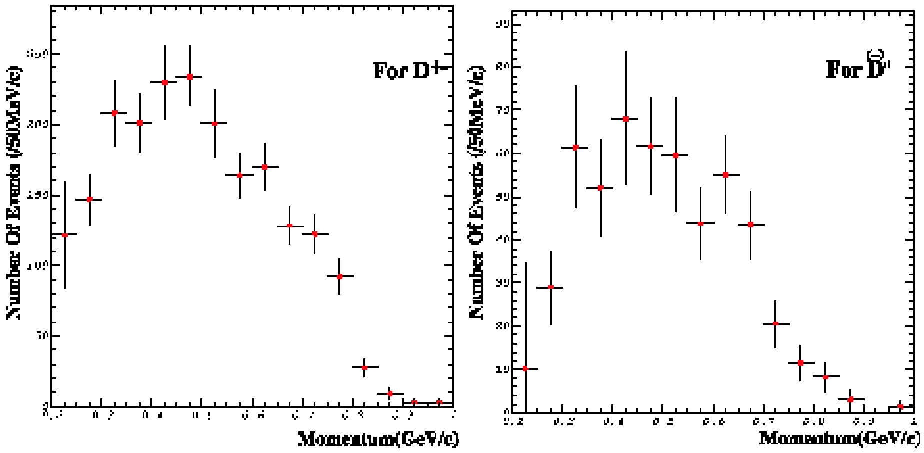

Figure 4: Inclusive electron spectra extracted from charged (left) and neutral (right) D meson decays.

the difficulties of soft muon identification.

Electron identification was optimized using radiative Bhabha events; key variables include E/p from the CsI and tracking along with dE/dx and RICH information. The preliminary results shown here use only one mode for each type of D meson ($K^-\pi^+$ and $K^-\pi^+\pi^+$). Even with this limitation and the modest data sample, the statistical uncertainties on the branching fraction are $\approx 0.6\%$ which can be compared with the current PDG world average of $(17.2 \pm 1.9\%)$. For the neutral case the CLEO-c has a similar statistical uncertainty, but here the PDG precision $(6.75 \pm 0.29\%)$ has not yet been reached. We hope to be able to reveal numbers for the actual branching fraction some time in Summer 2004. We must remember that this constitutes a small fraction of the data to be taken at this energy.

7 Exclusive Semileptonic D Decays

Exclusive semileptonic modes are also easily studied with the D tag technique. Here, we display signals using the variable $U \equiv E_{miss} - |p_{miss}|$, where E_{miss} (p_{miss}) denote the missing energy (momentum). This is computed by comparing the known beam energies to the sum of the D tag plus the observed particles in the semileptonic candidates. Clearly, U will peak at 0 if only a neutrino is missing.

Fig. 9 shows the U distributions for the Cabibbo-allowed $K^-e^+\nu_e$ final state, as well as the Cabibbo- suppressed $\pi^-e^+\nu_e$. Tagging allows one to separate the rarer π mode kinematically, rather than relying on particle identification alone. In Fig. 10, we display two other Cabibbo-suppressed modes, $\rho^0e^+\nu_e$ and $\rho^-e^+\nu_e$. The first of these has previously been seen, though not well-measured, whereas for the second this represents a first observation. Many other semileptonic modes are also accessible, and with the expected data set taken in the next year, CLEO-c can expect to produce the definitive results on 8 semi-leptonic D decays, with more to come later after the running at the D_s threshold.

8 Conclusion

We have shown the first results from the CLEO-c detector running at the $\psi(3770)$. The D mesons found from using the beam energy constraint are specularly clean, and can give large samples of *tagged* D events. One notable preliminary result is that of the D meson decay constant of $f_D = (230 \pm 42 \pm 10)$ MeV.

9 Acknowledgements

I would like to thank all my CLEO colleagues, but in particular Victor Pavluvin, Batbold Sanghi, Nabil Menaa, Laria Redjimi, Roy Briere and Basit Athar.

References

[1] M. Artuso *et al*, Nucl. Instrum. Methods A **502**, 91 (2003).

[2] Y. Kubota *et al*, Nucl. Instrum. Methods A **320**, 66 (1992).

[3] D. Peterson *et al*, Nucl. Instrum. Methods A **478**, 142 (2002).

[4] R.A. Briere *et al*, CLNS 01/1742, 2001.

[5] J. Adler *et al*, PRL 60, 89 (1988).

[6] G. Rong, on behalf of BES collaboration, hep-ex/0406027.

[7] L.Lellouch atnd C.J.Lin, Phys Rev **D64**, 094501 (2001).

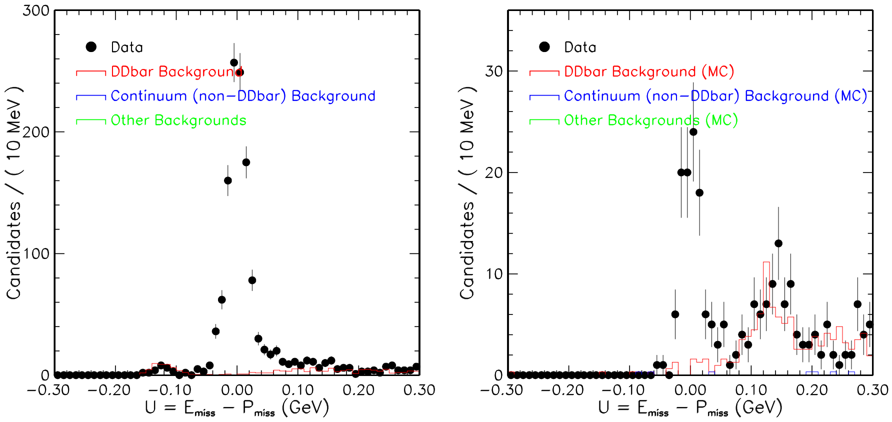

Figure 5: Distributions of $U \equiv E_{miss} - |p_{miss}|$ for the Cabibbo-allowed final state of $K^- e^+ \nu_e$ (left) and the Cabibbo-suppressed finat state $\pi^- e^+ \nu_e$ (right).

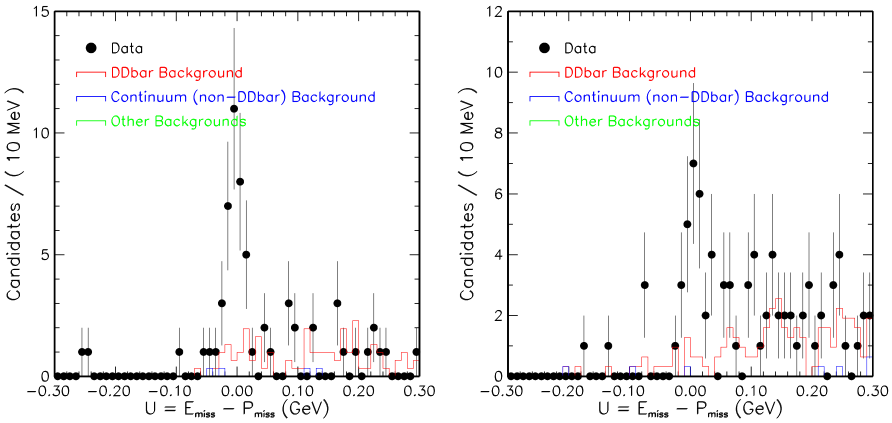

Figure 6: Distributions of $U \equiv E_{miss} - |p_{miss}|$ for the Cabibbo-suppressed states $\rho^0 e^+ \nu_e$ (left), and $\rho^- e^+ \nu_e$ (right).